

Geochemistry of low-temperature springs northwest of Yellowstone caldera: Seeking the link between seismicity, deformation, and fluid flow

William C. Evans^{a,*}, Deborah Bergfeld^a, Matthijs C. van Soest^b, Mark A. Huebner^a, John Fitzpatrick^a, Kinga M. Revesz^c

^a U.S. Geological Survey, 345 Middlefield Road, Menlo Park, CA 94025, USA

^b Lawrence Berkeley National Laboratory, Center for Isotope Geochemistry, Berkeley, CA 94701, USA

^c U.S. Geological Survey, Stable Isotope Laboratory, Reston, VA 20192, USA

Received 6 June 2005; received in revised form 22 December 2005; accepted 4 January 2006

Available online 10 March 2006

Abstract

A comprehensive geochemical survey of springs outside the northwest margin of the Yellowstone caldera was undertaken in 2003 and 2004. This survey was designed to detect: (1) active leakage from a huge reservoir of CO₂ gas recently postulated to extend from beneath the caldera into this area; and (2) lingering evidence for subsurface flow of magmatic fluids into this area during the 1985 seismic swarm and concomitant caldera subsidence. Spring temperatures are low (<15°C), but two large-discharge springs contain ¹⁴C-dead carbon that can be identified as magmatic from calculated end-member values for δ¹³C_(dead) and ³He/⁴He of -4‰ and 1 × 10⁻¹⁰, respectively, similar to values for intra-caldera fumarolic and hot-spring gases. However, the combined discharge of magmatic C is only 5.4 tonnes/day, <0.1% of the total output from Yellowstone. The two springs have slightly elevated ³He/⁴He ratios near 1 R_A and anomalous concentrations of Cl, Li, and B, and appear to represent minor leakage of gas-depleted, thermal waters out of the caldera. The small CO₂ signal detected in the springs is difficult to reconcile with a large underlying reservoir of gas in faulted and seismically active terrain. When considered with analyses from previous decades, the results provide no evidence to associate the ten-year period of caldera deflation that began in 1985 with expulsion of magmatic fluids through the caldera rim in this area.

Published by Elsevier B.V.

Keywords: Yellowstone National Park; magmatic gas; geochemistry; carbon dioxide; helium

1. Introduction

Interest in volcanic hazards at Yellowstone increased in 1975 when geodetic surveys showed that the central part of the caldera floor had risen ~1 m during the

previous 5 decades (Pelton and Smith, 1982). Uplift continued for several years, but subsidence was detected in 1985 (Dzurisin et al., 1994), and 0.25 m of subsidence occurred over the next 10 years (Wicks et al., 1998; Waite and Smith, 2002). In late 1985, a major seismic swarm began at the northwest caldera boundary. This swarm was unique among recorded events in that the epicenters gradually migrated away from the caldera for

* Corresponding author. Fax: +1 650 329 4463.

E-mail address: wcevans@usgs.gov (W.C. Evans).

several km to the northwest. The propagating seismicity coupled with caldera deflation pointed to subsurface fluid flow out of the caldera as the cause for both events (Waite and Smith, 2002; Fournier, 2004), but questions about the fluid and its role in the events remain. Magmatic brines, gases, and magma itself have all been invoked to account for Yellowstone's cycles of deformation and seismicity (Fournier, 1989; Dzurisin et al., 1994; Wicks et al., 1998; Waite and Smith, 2002; Wicks et al., 2002).

Negative anomalies in V_p and V_p/V_s recently detected in seismic tomographic imaging led Husen et al. (2004) to propose that a large reservoir of gas at depths as shallow as ~4 km below land surface extends from beneath the caldera to the northwest, in the same general area as the 1985 seismic swarm. They hypothesize that the gas is most likely CO_2 released from crystallizing magma beneath the caldera, and imply that migration of CO_2 -rich fluid might explain the propagating seismicity. Husen et al. (2004) note that CO_2 from such a shallow reservoir would likely leak to the surface and escape diffusely through soil, as occurred at Mammoth Mountain, California (Farrar et al., 1995).

A search for anomalous CO_2 emissions northwest of the caldera was warranted, but detecting anomalous efflux over large regions of wilderness and in the absence of clear vegetation kills is logistically daunting. We chose instead to search for dissolved magmatic C in springs and streams, because CO_2 is fairly soluble in cold water. High-pressure CO_2 has been implicated in propagating seismic swarms at Mammoth Mountain USA (Hill and Prejean, 2005), Colfiorito Italy (Miller et al., 2004; Chiodini et al., 2004), and the Eger rift in central Europe (Bräuer et al., 2003). Springs with highly anomalous concentrations of magmatic C are long-lived and conspicuous features in these areas (Sorey et al., 1998; Chiodini et al., 1999; Bräuer et al., 2003). An advantage to collecting waters is that the samples can be analyzed for other magmatic or hydrothermal species of interest (e.g., He, Cl); and because the study area was included in previous regional geochemical studies, we can evaluate whether any chemical anomalies could be related to the 1985 seismic swarm and ensuing subsidence.

2. Study area, sampling logistics, and methods

The study area (Fig. 1) extends to the north and west from Terrace Spring, a sub-boiling hot spring located near the caldera rim 14 km southwest of Norris, and covers the location of the 1985 seismic swarm, the

general region of elevated seismicity trending through the Madison Valley, and a substantial part of the hypothesized gas reservoir of Husen et al. (2004). The study area includes numerous normal faults (Christiansen, 2001) and encompasses the discharge area for groundwaters draining from the northwest caldera rim to provide the best chances of detecting any Yellowstone fluids forced out beneath this part of the rim that then rise toward the surface.

Paleozoic and Mesozoic marine sedimentary rocks (shaded green in Fig. 1) are exposed in the northern part and to the west of the study area. Cenozoic volcanic rocks, Precambrian gneisses and schists and alluvium occupy the rest of the study area (Christiansen, 2001; O'Neill and Christiansen, 2004). The contrasting geology is clearly reflected in calcium and magnesium concentrations of spring waters. The products of Yellowstone volcanism are predominantly rhyolites that are exceptionally low in both elements, whereas limestone and dolomite are common in the sedimentary rocks to the north (Christiansen, 2001; Hildreth et al., 1991).

Annual precipitation in the study area averages about 1 m/year with up to 30% recharge (Kharaka et al., 2002), feeding a voluminous groundwater flow that could easily dilute magmatic or hydrothermal inputs to trace concentrations. The strategy adopted to search for anomalies was to measure the specific conductance of streams at low elevations in their drainages, and if conductance was abnormally high, to move upstream to the source springs and sample those with the highest conductance. Increased conductance can potentially reflect chloride input from thermal waters or HCO_3^- generated from magmatic CO_2 . Many of the springs in the study area actually consist of clusters of distinct vents. The field conductance measurements indicated whether all of the vents discharged similar fluids. At two of the springs, Black Sand and Big Springs, vents showed a significant range in temperature and conductance, and two vents that spanned the range were sampled at each of these vent clusters.

Many springs and streams were visited but not sampled if conductivity, temperature, or pH measurements indicated no anomalies. Flow rate, determined from visual estimates or direct gaging, and areal distribution were also used to select sample sites. Large-discharge springs were especially targeted because their recharge zones cover more of the study area, and they represent a greater total flux for a given concentration anomaly than do low-discharge springs. Known spring areas around the alluvium-filled Madison Valley were visited as were most streams flowing into the valley from the north and east (Fig. 1) to provide

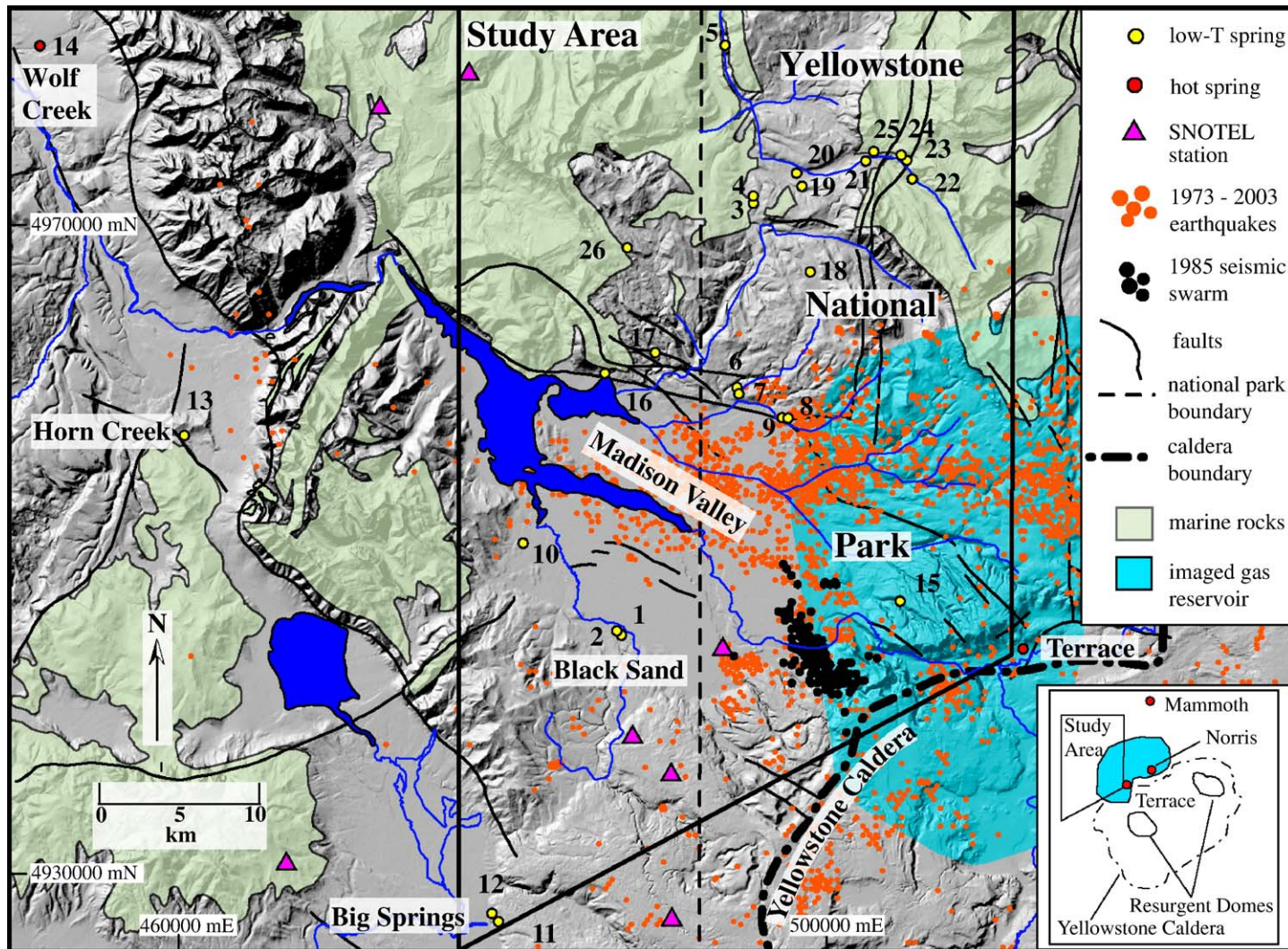
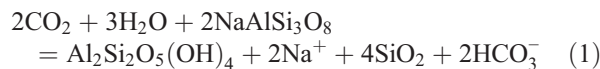


Fig. 1. Map of region showing study area, water collection sites, and other features of interest. Geology generalized from Christiansen (2001) and O'Neill and Christiansen (2004). Gas extent at 2 km bsl from $V_p/V_s \leq 1.6$ (Husen et al., 2004).

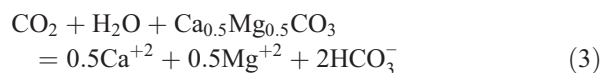
coverage of the seismically active area and the drainage from the region above the gas reservoir, an upland recharge area where few springs emerge. Sampled springs in the sedimentary rocks are more remote, but some are near the inferred extension of normal faults that trend north from the area of seismicity. Samples were also collected from Wolf Creek hot spring and a low-temperature spring on Horn Creek. These sites are far to the west of the study area with no obvious hydrologic connection to Yellowstone.

Emphasis was placed on sampling for helium, carbon, and their isotopic ratios. For helium, samples of water (and gas bubbles, if present) were collected in 10-cm³ Cu tubes sealed at both ends with refrigeration clamps. Samples were analyzed at the Lawrence Berkeley National Laboratory following procedures discussed in Kennedy et al. (1985) and Hiyagon and Kennedy (1992). Carbon isotope analyses were performed on the total dissolved inorganic carbon (DIC), which comprises CO₂, HCO₃⁻, and CO₃²⁻. Samples of water for DIC analysis were collected in pre-evacuated Pyrex bottles and acidified to convert all the DIC into CO₂ for later extraction.

Studies of carbon in groundwater focus on DIC because some fraction of the CO₂ (from any source) that is absorbed by the water is converted to HCO₃⁻ and CO₃²⁻ through water–rock interaction. In volcanic or crystalline rocks, this occurs through silicate hydrolysis, for example:



Other silicate minerals contribute K⁺ and Ca²⁺ in similar reactions. In carbonate rocks, Ca²⁺ and Mg²⁺ can be released by dissolution, for example:



In reaction (3), the molar DIC increases two-fold, and the carbon isotopes reflect the mixture of carbon sources. To help distinguish waters influenced by carbonate dissolution, samples of water were filtered and acidified

Table 1

Water chemistry and basic parameters. Site numbers correspond to map in Fig. 1. “(C)” and “(N)” signify carbonate and non-carbonate rocks in the drainage areas. Boldface values from 2004. Analytical precision is ±5% for dissolved species. “HCO₃⁻” is alkalinity as bicarbonate

No.	Name (drainage geology)	<i>T</i>	cond.	pH	O ₂	Na	K	Ca	Mg	SiO ₂	Li	B	Cl	SO ₄	HCO ₃
		(°C)	(μS/cm)		(mg/L)			(μg/L)			(mg/L)				
1	Black Sand Spr. east (N)	10.1	105	7.04	7.6	13.2	1.8	5.0	0.8	36.0	50.0	90	5.1	1.4	39
2	Black Sand Spr. west (N)	8.2	83.7	7.12	7.8	8.9	1.7	5.0	1.0	32.7	35.1	60	3.1	1.3	33
3	Pass Crk. spr. A (C)	7.1	251	7.92	4.9	1.1	0.7	33.9	7.9	8.8	1.5	<20	0.41	5.3	158
4	Pass Crk. spr. B (C)	5.8	292			1.1	0.6	43.7	7.4	10.7	1.1	<20	0.41	3.8	190
5	lower Gallatin R. spr. (C)	6.6	294	8.16	5.2	1.6	0.9	31.8	14.3	11.4	2.3	<20	0.63	20.8	171
6	Campanula Crk. spr. (N)	6.8	129	7.25	5.8	3.9	1.4	14.2	3.4	28.8	3.0	<20	1.03	2.0	74
7	Campanula Crk. (N)	7.7	60.6			2.9	1.0	5.7	1.4	15.1	1.4	<20	0.42	1.7	34
8	Gneiss Crk. spr. (N)	5.6	63.3	6.89	6.1	3.1	0.8	6.0	1.3	20.9	1.8	<20	0.60	1.9	34
9	Gneiss Crk. (N)	12.9	94.7			5.6	1.2	9.1	1.8	16.8	1.4	<20	0.46	3.6	52
10	Basin Cabin Spr. (N)	7.0	145	7.32	6.0	4.5	1.1	14.8	4.2	20.9	4.8	<20	1.62	3.1	74
11	Big Spr. south (N)	13.4	131	6.74	7.3	16.3	3.1	4.6	0.7	43.3	73.7	80	4.1	2.8	56
12	Big Spr. north (N)	10.6	98.0	6.86	8.2	12.0	2.6	4.4	0.8	38.5	53.2	50	3.0	2.3	45
13	Horn Crk spr. (C)	8.5	284	8.11	8.7	6.0	1.5	23.8	14.6	15.6	7.6	<20	2.6	3.2	179
14	Wolf Crk. hot spr. (N)	58.7	534	9.81		95.1	1.5	3.0	0.4	46.3	73.7	40	21.0	49	170
15	Mt. Jackson spr. (N)	7.4	51.0	6.42	8.6	3.6	1.1	3.7	0.7	29.7	10.4	<20	1.03	1.9	21
16	Corey Spr. (C)	7.7	425	7.92	4.3	1.5	0.8	41.3	21.6	7.5	3.2	<20	0.64	83	187
17	lower Whits Lk. spr. (N)	5.1	68.7	7.15	9.4	3.5	1.5	5.8	1.2	21.6	3.2	<20	0.56	6.1	31
18	Grayling Crk. spr. (N)	4.1	28.0	7.04	9.9	2.0	0.8	1.8	0.5	19.5	1.0	<20	0.43	1.7	13
19	Gallatin R. spr. A (C)	4.3	171	7.81	9.8	1.9	1.3	20.2	5.2	21.4	1.2	<20	0.51	1.7	105
20	Gallatin R. (C)	8.7	392			1.0	0.4	44.1	17.3	4.5	1.6	<20	0.35	86	160
21	Gallatin R. spr. B (C)	4.6	251	8.13	6.8	0.5	0.4	25.2	13.1	4.1	0.8	<20	0.37	8.5	154
22	upper Gallatin R. (C)	9.8	273			0.4	0.3	31.8	12.5	3.0	<0.3	<20	0.33	4.7	178
23	upper Gallatin R. spr. A (C)	3.6	457	8.08	7.5	0.7	0.4	50.9	19.9	3.9	1.7	<20	0.33	113	154
24	upper Gallatin R. spr. B (C)	4.6	693	7.82	3.6	1.3	<1.0	84.6	34.5	4.0	<9.0	<400	0.40	240	160
25	Gallatin R. mineral spr. (C)	7.4	2310	7.41	3.4	3.1	<1.0	492	34.3	5.0	<9.0	<400	0.53	1300	263
26	Tepee Crk. spr. (C)	3.6	102	7.01	8.9	1.8	1.1	14.5	1.7	20.7	0.9	2	0.33	1.7	57

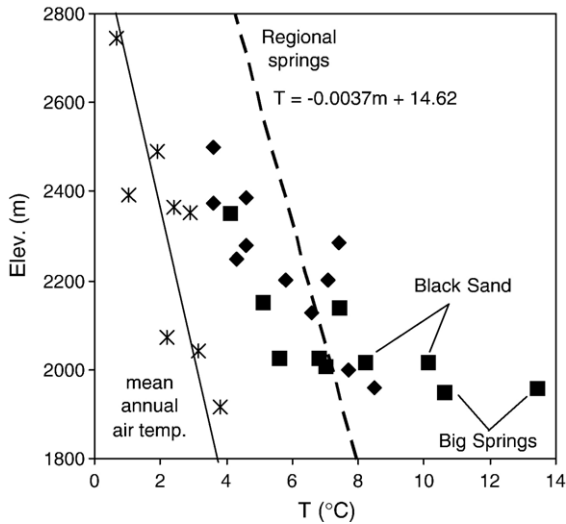


Fig. 2. Measured spring temperatures compared to mean annual air temperatures 1999–2004 (asterisks) in and around the study area and to the dashed regression line through 56 dilute ($Cl < 2$ mg/L), low-temperature springs in the greater Yellowstone region (Kharaka et al., 2002). Diamonds: springs draining carbonate rocks; squares: springs draining non-carbonate rocks. Air temperatures from SNOTEL stations (<http://www.wcc.nrcs.usda.gov/snow/>).

for cation analysis. Filtered water for anion analysis was not acidified. Further details of all the sampling procedures are described in Evans et al. (2002).

The $\delta^{13}C$ -DIC and ^{14}C -DIC were determined using purified CO_2 extracted from the DIC tubes. The $\delta^{13}C$ analyses (and δD and $\delta^{18}O$) were run at USGS laboratories in Reston Virginia and Menlo Park California; ^{14}C analyses were run at the CAMS facility at Lawrence Livermore National Laboratory.

3. Results

All but one of the features were sampled in August 2003. Several sites were revisited in September 2004 to check for annual variability and to fill in data gaps. Results from revisited sites showed remarkable similarity to the 2003 values, within measurement uncertainty for nearly every parameter checked.

Chemical analyses are given in Table 1. The low-temperature springs show an inverse relation between temperature and elevation but are warmer than mean annual air temperatures measured at local SNOTEL stations (Fig. 2). Most spring temperatures conform reasonably well to the trend defined by 56 dilute ($Cl < 2$ mg/L), low-temperature springs in the greater Yellowstone region reported by Kharaka et al. (2002). Black Sand and Big Springs, however, have vent temperatures that are 1–5°C higher than expected

when compared to either the regional trend or the other springs in this study.

The pH and dissolved oxygen values are typical for low-temperature groundwaters (Table 1). The pH values are all in the neutral range, showing that HCO_3^- makes up more than half of the DIC as a result of reactions like those in Eqs. (1)–(3). Dissolved oxygen concentrations are between 3 and 10 mg/L, corresponding to about 30–100% of saturation with atmospheric O_2 at the measured spring temperatures.

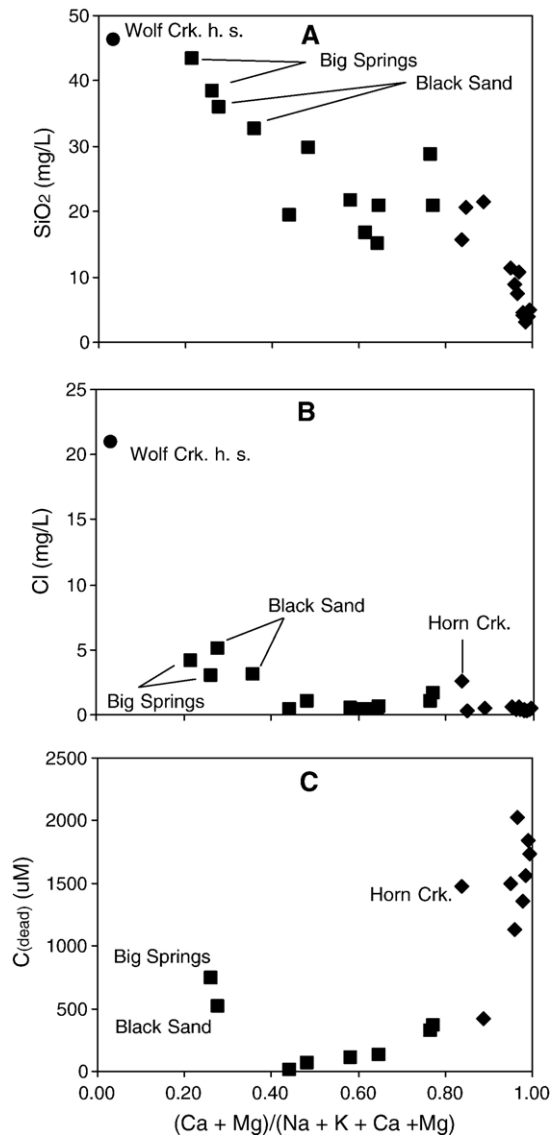


Fig. 3. (A) Silica vs. fraction (Ca+Mg). Springs draining carbonate (diamonds) and non-carbonate rocks (squares). (B) Cl vs. fraction (Ca+Mg). Springs draining carbonate (diamonds) and non-carbonate rocks (squares). (C) Dead carbon (see text) vs. fraction (Ca+Mg). Springs draining carbonate (diamonds) and non-carbonate rocks (squares).

Several aspects of the spring chemistry reflect geologic setting. The springs draining areas of marine sediments typically have specific conductances $>150\mu\text{S}/\text{cm}$. These springs tend to be low in SiO_2 but high in Ca and Mg, which constitute $>80\%$ of the cations, reflecting the dominance of dissolution reactions such as Eq. (3). Some of these springs are high in SO_4^{2-} , no doubt resulting from gypsum-or anhydrite-bearing units in the carbonate rocks (Plummer et al., 1990; Christiansen, 2001). One of the springs (#25) is sufficiently concentrated to deposit a mineral apron around the vent. Springs not draining marine sediments typically are dilute, with specific conductances $<150\mu\text{S}/\text{cm}$, but have higher SiO_2 concentrations and tend to be mixed-cation waters.

Black Sand and Big Springs are Na-K dominated and relatively high in SiO_2 (Fig. 3A). Both springs have Li, B, and Cl concentrations that are higher than the other

low-temperature springs (Table 1). These characteristics and the warmer temperatures all point to a small component of thermal fluid. Excluding these two springs, the background Cl concentration in non-thermal groundwater within the study area seems independent of surface geology (Fig. 3B) and averages about $0.5\text{mg}/\text{L}$, similar to the $0.7\text{mg}/\text{L}$ background proposed by Ingebritsen et al. (2001) for the entire park.

The gas from the bubbling springs was dominated (98–99%) by the air gases $\text{N}_2 + \text{O}_2 + \text{Ar}$, as expected for spring waters that equilibrate with the atmosphere at recharge. Minor amounts of CO_2 made up most of the balance, although variable enrichments in He were also noted.

Isotopic results are presented in Table 2. The range in δD and $\delta^{18}\text{O}$ values is similar to that found in the previous survey of Kharaka et al. (2002). All the waters plot near the global meteoric water line, but neither δD nor $\delta^{18}\text{O}$ correlates with spring elevation. The lack of

Table 2

Isotopic ratios and dissolved inorganic carbon (DIC). Site numbers correspond to map in Fig. 1. “(C)” and “(N)” signify carbonate and non-carbonate rocks in the drainage areas. Boldface values from 2004. Helium isotope values in italics are from gas bubbles. Analytical precision is $\pm 1\%$ for δD , $\pm 0.1\%$ for $\delta^{18}\text{O}$ and $\delta^{13}\text{C}$, ± 0.5 percent-modern carbon (pmC) for ^{14}C , and $\pm 5\%$ for DIC. Individual $1-\sigma$ uncertainties are given for $^3\text{He}/^4\text{He}$. Air ratios (R_A) = 3.12 for $^4\text{He}/^{22}\text{Ne}$ and 1.40×10^{-6} for $^3\text{He}/^4\text{He}$

No.	Name (drainage geology)	δD SMOW	$\delta^{18}\text{O}$ SMOW	$\delta^{13}\text{C}$ PDB	^{14}C pmC	DIC mM	$C_{(\text{dead})}$ mM ^a	$^4\text{He}/^{22}\text{Ne}$ R/R _A	$^3\text{He}/^4\text{He}$ R/R _A	σ	$(^3\text{He}/\text{C})_t$ ^b	$(^3\text{He}/\text{Cl})_t$ ^c
1	Black Sand Spr. east (N)	-140	-18.8	-8.9	42.4	0.82	0.52	<i>14.8</i> ; 20.1	<i>0.95</i> ; 0.97	<i>0.03</i> ; 0.03	1×10^{-10}	4×10^{-10}
2	Black Sand Spr. west (N)	-138	-18.6									
3	Pass Crk. spr. A (C)	-139	-18.6	-10.5	64.2	2.56	1.13					
4	Pass Crk. spr. B (C)	-138	-18.5									
5	lower Gallatin R. spr. (C)	-144	-19.2	-8.7	52.2	2.75	1.50	<i>1.08</i>	<i>1.61</i>	<i>0.03</i>	1×10^{-12}	6×10^{-10}
6	Campanula Crk. spr. (N)	-144	-19.0	-14.6	87.1	1.34	0.33					
7	Campanula Crk. (N)	-136	-18.1									
8	Gneiss Crk. spr. (N)	-140	-18.6	-16.9	95.9	0.79	0.13	<i>0.99</i>	<i>1.09</i>	<i>0.08</i>	1×10^{-12}	7×10^{-11}
9	Gneiss Crk. (N)	-137	-18.3									
10	Basin Cabin Spr. (N)	-140	-18.6	-14.2	85.2	1.43	0.37	2.10	1.14	0.07	1×10^{-11}	2×10^{-10}
11	Big Spr. south (N)	-136	-18.4	-7.0		1.38	1.01 ^d	29.20	1.21	0.03	1×10^{-10}	1×10^{-9}
12	Big Spr. north (N)	-136	-18.3	-7.9	31.1	1.02	0.75	<i>20.4</i>	<i>1.19</i>	<i>0.03</i>	7×10^{-11}	8×10^{-10}
13	Horn Crk spr. (C)	-145	-19.0	-9.1	58.8	3.03	1.48	16.2	0.33	0.02	9×10^{-12}	2×10^{-10}
14	Wolf Crk. hot spr. (N)	-151	-19.9	-5.5		2.36		<i>2730</i>	<i>0.15</i>	<i>0.01</i>		
15	Mt. Jackson spr. (N)	-146	-19.2	-14.7	95.6	0.39	0.07	1.22	1.06	0.1	2×10^{-11}	1×10^{-10}
16	Corey Spr. (C)	-144	-19.3	-6.8	41.5	3.17	2.02					
17	lower Whits Lk. spr. (N)	-138	-18.3	-13.4	93.6	0.60	0.11					
18	Grayling Crk. spr. (N)	-139	-18.5	-13.8	109	0.25	0.01					
19	Gallatin R. spr. A (C)	-141	-18.8	-12.4	89.1	1.87	0.42					
20	Gallatin R. (C)	-138	-18.8									
21	Gallatin R. spr. B (C)	-139	-18.7	-7.6	52.5	2.50	1.36					
22	upper Gallatin R. (C)	-137	-18.5									
23	upper Gallatin R. spr. A (C)	-142	-19.1	-7.6	48.3	2.70	1.57	1.78	0.79	0.17	1×10^{-12}	n.a.
24	upper Gallatin R. spr. B (C)	-144	-19.2	-6.7	36.5	2.70	1.84					
25	Gallatin R. mineral spr. (C)	-141	-18.6	-10.7	72.5	4.69	1.74	<i>1.41</i>	<i>1.08</i>	<i>0.04</i>	7×10^{-13}	1×10^{-9}
26	Tepee Crk. spr. (C)			-13.0		0.99						

^a $C_{(\text{dead})} = \text{DIC}(1 - ^{14}\text{C}/115)$.

^b End-member thermal water component calculated as: ^3He in excess of the amount in 5°C ASW divided by $C_{(\text{dead})}$.

^c End-member thermal water component calculated as: ^3He in excess of the amount in 5°C ASW divided by the Cl in Table 1-less $0.5\text{mg}/\text{L}$ background.

^d Assumes same ^{14}C as Big Springs north.

correlation has been noted previously and probably stems from complexities in storm tracks and topography (Kharaka et al., 2002) and a marked difference in recharge season between low and high elevations (Despain, 1987). The isotopes of the DIC show a large range of values in both $\delta^{13}\text{C}$ (–16.9‰ to –6.7‰) and ^{14}C (31–109 pmC), reflecting both biogenic and abiogenic contributions. $^3\text{He}/^4\text{He}$ ratios show a relatively narrow range with a cluster of values near $1R_A$ (where “ R_A ” means “ratio in air” of two isotopes).

4. Discussion

4.1. Carbon sources

Young (<50 years old) groundwaters that contain only C dissolved at recharge from biogenic sources such as soil respiration or from the atmosphere should have ^{14}C values ≥ 100 percent modern carbon (pmC) due to the bomb effect. One of our sampled springs (#18) shows this enrichment (Table 2), but all other springs show some depletion in ^{14}C , due to addition of “dead” C from carbonate minerals or magmatic sources. To calculate the concentration of dead DIC (C_{dead} in Table 2), we assume that the biogenic DIC contains 115 pmC, the average ^{14}C value in the atmosphere 1–2 decades ago, which allows a reasonable circulation time for the groundwater (see James et al., 1999; Evans et al., 2004). The probable error in this assumption is small compared to the uncertainties inherent in distinguishing marine carbonate from magmatic sources of the dead carbon.

The mixed-cation waters (40–80% Ca+Mg) draining non-carbonate terrains contain very little C_{dead} from any source (Fig. 3C). Although some or all of this C_{dead} could be magmatic, the slight increase in C_{dead} with increasing Ca+Mg suggests that some form of carbonate (e.g., glacially redistributed marine rocks, soil carbonates, etc.) may have dissolved in the water. Waters with >80% Ca+Mg have substantially more C_{dead} , as expected from reaction with the local marine carbonate rocks. Black Sand and Big Springs contain C_{dead} that is not likely derived from marine carbonates given that these springs are rich in Na+K and issue from non-carbonate terrains. A magmatic origin for this C_{dead} is plausible.

Marine and magmatic carbon sources can be distinguished in principle using $\delta^{13}\text{C}$ values. Magmatic C at Yellowstone should be characterized by the $\delta^{13}\text{C}$ values of the CO_2 released from hot springs and fumaroles within the caldera, which range from –2.5‰ to –4.9‰ in recent analyses from Werner and

Brantley (2003). The $\delta^{13}\text{C}$ values of marine carbonate rocks in the northern Yellowstone area are higher and range from –2.3‰ to +3.3‰ (Friedman, 1970). The mixture of atmospheric and biogenic CO_2 that dissolves into waters at recharge can vary over a wide range of $\delta^{13}\text{C}$ values, depending on vegetation type and other factors in the recharge areas, but is certain to be substantially lighter than either marine or magmatic carbon. Amundson and Davidson (1990) suggest a maximum $\delta^{13}\text{C}$ value of ~ -9 ‰ for this component.

Fig. 4 shows $\delta^{13}\text{C}$ plotted against ^{14}C for all the low-temperature springs where ^{14}C was analyzed. The general trend of increasing $\delta^{13}\text{C}$ with decreasing ^{14}C is clear, but it also appears that the springs in carbonate and non-carbonate rocks follow slightly different trends. A trend line through the springs in carbonate terrains is consistent with an end-member $\delta^{13}\text{C}$ value of –1‰ for the C_{dead} , within the range of local carbonate rocks. This well-defined trend greatly strengthens the evidence for magmatic carbon in Black Sand and Big Springs, which plot on a trend line indicating a $\delta^{13}\text{C}$ value of –4‰ for the C_{dead} . Because of the large variability in the $\delta^{13}\text{C}$ value of the biogenic end member, the source of C_{dead} in springs that show slight ^{14}C depletion (80–100 pmC) is poorly constrained by this plot.

4.2. Helium isotopes

Infiltrating water absorbs atmospheric He, but the low concentration of He in air (0.0005%) and its low aqueous solubility lead to a small initial concentration in groundwater. Addition of He from any other source can be easily recognized by an increase in the ratio of ^4He to ^{22}Ne , an isotope almost wholly derived from the

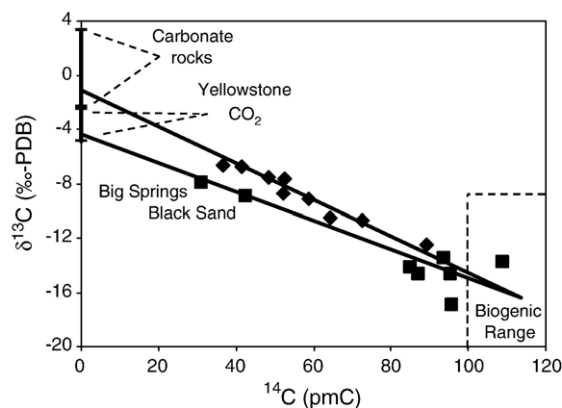


Fig. 4. $\delta^{13}\text{C}$ vs. ^{14}C of the DIC. Springs draining carbonate (diamonds) and non-carbonate rocks (squares) with trend lines. $\delta^{13}\text{C}$ of local carbonate rocks from Friedman (1970); Yellowstone CO_2 from (Werner and Brantley, 2003).

atmosphere (Kennedy et al., 1985). The ratio of $^4\text{He}/^{22}\text{Ne}$ in air-saturated water (ASW) at 5°C is $0.78R_A$ due to the slightly greater solubility of Ne relative to He. Spring waters with He from any non-atmospheric source should have $^4\text{He}/^{22}\text{Ne}$ values $>0.78R_A$. Magmatic He input to groundwater will also increase the $^3\text{He}/^4\text{He}$ ratio. $^3\text{He}/^4\text{He}$ ratios reach $7\text{--}8R_A$ in many Yellowstone thermal areas, and a few values as high as $16\text{--}17R_A$ have also been recorded (Kennedy et al., 1985; Werner and Brantley, 2003).

The measured $^4\text{He}/^{22}\text{Ne}$ and $^3\text{He}/^4\text{He}$ ratios, each normalized to its respective R_A , are given in Table 2. Wolf Creek hot spring shows a huge He enrichment and a low $^3\text{He}/^4\text{He}$ ratio, suggesting that the major He source is crustal, radiogenic production during a long, deep fluid circulation path. Horn Creek spring, located outside of the Yellowstone area and closer to Wolf Creek, shows considerable helium enrichment and also has a low $^3\text{He}/^4\text{He}$ ratio. Many of the low-temperature springs in the study area show some He enrichment and have higher $^3\text{He}/^4\text{He}$ ratios near $1R_A$, but none approach the magmatic range ($\geq 7R_A$).

In Fig. 5, the normalized $^4\text{He}/^{22}\text{Ne}$ ratios for gas-bubble samples have been multiplied by 0.78 to reduce the solubility-induced bias between the two types of samples. The inverse scale on the x-axis allows straight-line extrapolations from ASW through the sample points to indicate the $^3\text{He}/^4\text{He}$ ratio of the added He on the y-axis. One spring shows a small enrichment along the “magmatic” He line, but the end-member (y-axis) values

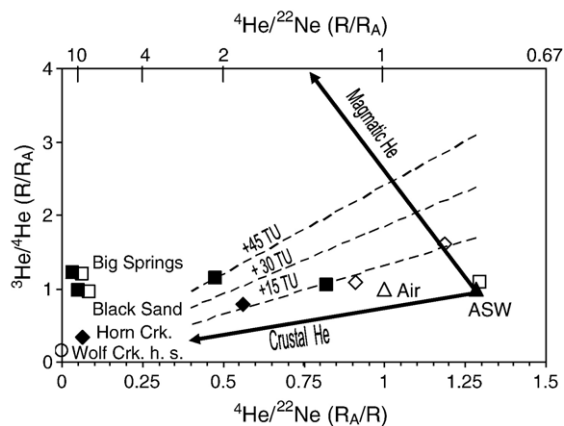


Fig. 5. Air-normalized $^3\text{He}/^4\text{He}$ vs. $^4\text{He}/^{22}\text{Ne}$ (reciprocal scale at bottom). Springs draining carbonate (diamonds) and non-carbonate rocks (squares) with filled symbols for water samples, open symbols for gas samples (for which $^4\text{He}/^{22}\text{Ne}$ (R/R_A) was multiplied by 0.78). Arrows show the effects of adding magmatic ($\geq 7R_A$) and crustal ($\approx 0.01R_A$) helium to air-saturated water. Dashed lines show the potential effects of tritium decay on air-saturated water enriched in crustal helium.

for the rest of the low-temperature springs in the study area are between 0.6 and $1.3R_A$. These values could reflect some mixture of magmatic and crustal He, but for the low levels of He enrichment in most of these springs, could also reflect addition of ^3He from tritium decay as shown in Fig. 5 (see Saar et al., 2005). For groundwaters that might have residence times of a few decades, decay of up to 45 tritium units (TU) is possible (see: Pearson and Truesdell, 1978). However, Black Sand and Big Springs require a magmatic He input, as decay of $>500\text{ TU}$ would be needed without it. Thus, both the helium and carbon isotope data imply a magmatic volatile input to these two springs, and allow but do not prove, tiny magmatic inputs to some of the other springs.

4.3. $^3\text{He}/\text{C}$ and $^3\text{He}/\text{Cl}$ ratios

Molar ratios of $^3\text{He}/\text{C}$ and $^3\text{He}/\text{Cl}$ can provide more information on any magmatic/hydrothermal component in the springs if the atmospheric and biogenic inputs and the non-thermal Cl are factored out. The total ^3He dissolved in the low-temperature spring waters is calculated as the product of the $^3\text{He}/^4\text{He}$ and $^4\text{He}/^{22}\text{Ne}$ ratios and the assumed ^{22}Ne concentration in 5°C ASW (the error due to temperature is small over the observed range). Subtracting the ^3He acquired at recharge (calculated for 5°C ASW) leaves the concentration of non-atmospheric ^3He . Dividing the result by $C_{(\text{dead})}$ gives $(^3\text{He}/\text{C})_t$, the ratio pertinent to the deep thermal component (but including tritogenic ^3He). The analogous $(^3\text{He}/\text{Cl})_t$ ratio is calculated after reducing the Cl concentrations in Table 1 by 0.5 mg/L assumed as a background value.

Interestingly, Black Sand and Big Springs have $(^3\text{He}/\text{C})_t$ ratios of 10^{-10} (Table 2). This ratio is the characteristic order of magnitude for magmatic gas (see e.g., Hilton et al., 2002) and is near the molar $^3\text{He}/\text{C}$ ratio of 3×10^{-10} in recent gas analyses for several hot springs and fumaroles in Yellowstone (Werner and Brantley, 2003). The similarity in ratios suggests that the thermal-fluid component in Black Sand and Big Springs is leakage from the Yellowstone system. Other springs have substantially lower values (Table 2). Those springs in sedimentary terrains have $(^3\text{He}/\text{C})_t$ values $\leq 10^{-12}$, consistent with derivation of $\geq 99\%$ of the $C_{(\text{dead})}$ from carbonate rocks.

A characteristic $^3\text{He}/\text{Cl}$ ratio for Yellowstone cannot be obtained from discrete samples because the presence of both vapor-dominated (acid sulfate) and liquid-dominated (neutral chloride) zones leads to geographic separation of gas ($^3\text{He} + \text{CO}_2$) and salt discharges

(Fournier, 1989). However, a $^3\text{He}/\text{Cl}$ ratio representative of the deep, unboiled parent fluid can be calculated from total emissions. Total ^3He emissions from Yellowstone can be obtained from the $^3\text{He}/\text{C}$ ratio (3×10^{-10}) and total magmatic C emissions. Werner and Brantley (2003) estimated the total diffuse emission of CO_2 from Yellowstone, within and outside the caldera, at 45,000 tonnes/day, and argue that this value should approximate the total magmatic C flux. Ingebritsen et al. (2001) derived a total hydrothermal Cl flux of 1740 g/s in rivers draining from the caldera region, the Norris-Mammoth corridor (Sorey, 1991), and the Bechler River-Boundary Creek area (Parry and Bowman, 1990). The molar $^3\text{He}/\text{Cl}$ ratio obtained by combining these estimates is 7×10^{-8} .

The total hydrothermal Cl flux is well constrained (Ingebritsen et al., 2001), but an order of magnitude error in this calculated $^3\text{He}/\text{Cl}$ might result from uncertainties in the $^3\text{He}/\text{C}$ ratio and the total magmatic C emissions. Still, the $(^3\text{He}/\text{Cl})_t$ ratios in springs we sampled, including Black Sand and Big Springs, are less than the Yellowstone ratio by factors of 70–1000 (Table 2), implying that the thermal fluid leaking into the study area is gas-poor, probably depleted in gas content because of prior vapor loss as depicted in Fig. 6. If the thermal fluid were enriched in magmatic gases, diffusive loss of He from the groundwaters prior to discharge would also produce low $(^3\text{He}/\text{Cl})_t$ ratios, but

this process does not explain why the $^3\text{He}/^4\text{He}$ ratios are much lower than typical magmatic values. Addition of radiogenic ^4He can more readily lower the $^3\text{He}/^4\text{He}$ ratio in waters that are gas poor and low in total He, a fact used previously to explain some of the $^3\text{He}/^4\text{He}$ variations between thermal features at Yellowstone (Kennedy et al., 1987; Fournier, 1989).

4.4. Total heat and mass transport

The total flow of all the springs sampled or field-checked within the study area is $\sim 8\text{--}10\text{ m}^3/\text{s}$. Using the maximum recharge estimate by Kharaka et al. (2002) of 0.3 m/year, the minimum recharge area required to account for this flow is $800\text{--}1000\text{ km}^2$, at least half the size of the 1600 km^2 study area. Although much of the recharge for Big Springs likely occurs outside of the study area, our sampling coverage of the groundwater system would seem to be reasonably complete, given that streams were also field-checked at base-flow conditions.

Our results on spring chemistry provide no evidence for diffuse efflux of magmatic CO_2 in the study area. The concentration of $\text{C}_{(\text{dead})}$ exceeds 1 mM only in those springs located in areas of sedimentary rocks, where chemistry, carbon isotopes and $(^3\text{He}/\text{C})_t$ all favor a carbonate source for most of the dead carbon (Table 2; Figs. 3C and 4). Globally, areas of diffuse degassing of magmatic CO_2 also host groundwaters rich in DIC. This occurs because the Ostwald coefficient for CO_2 is > 1 at temperatures below 15°C (Wilhelm et al., 1977), causing preferential partitioning of CO_2 into solution. Examples include Furnas volcano in Azores (Cruz et al., 1999) and many locations in central Italy (Chiodini et al., 1999), as well as at Mammoth Mountain California, where low-temperature springs contain 20–50 mM magmatic CO_2 and have elevated $^3\text{He}/^4\text{He}$ ratios of $3\text{--}5R_A$ (Evans et al., 2002).

Assuming that no anomalous discharges (dissolved or diffuse) escaped detection, the total output of magmatic carbon, hydrothermal Cl, and heat in the study area can be calculated. These totals can be derived with little error from only the Black Sand and Big Springs results because the Cl and magmatic C anomalies are small in the other springs.

In wet climates, the temperature anomaly of spring water is customarily referenced to mean annual air temperature (see, e.g., Nathenson et al., 2003), sometimes corrected for the estimated elevation drop between recharge and discharge (Manga, 2001). Fig. 2 shows that mean annual air temperature is clearly not the correct reference for the climatic conditions around

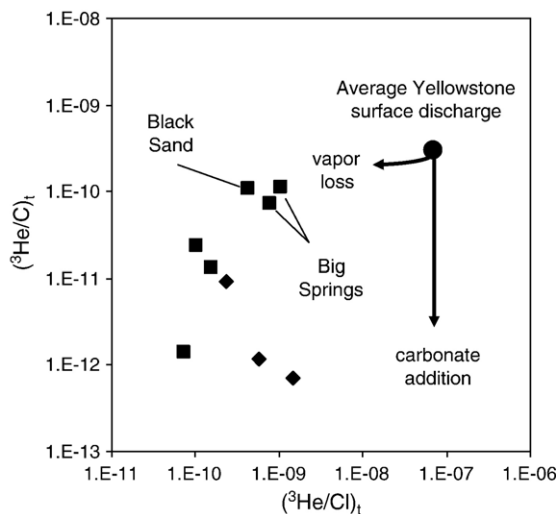


Fig. 6. $^3\text{He}/\text{C}$ vs. $^3\text{He}/\text{Cl}$ in the low-temperature springs corrected for biogenic and atmospheric contributions other than tritium (see text). Springs draining carbonate (diamonds) and non-carbonate rocks (squares). Black Sand and Big Springs can be related to Yellowstone fluids through vapor loss with slight fractionation of He/C. Other springs require an additional carbon source and may also contain tritogenic ^3He instead of Yellowstone fluid components.

Yellowstone, but the trend line developed from the Kharaka et al. (2002) data can be used. Average Black Sand water is $\sim 2^\circ\text{C}$ warmer, and average Big Springs water $\sim 4.5^\circ\text{C}$ warmer, than the trend-line temperature at the discharge elevation. For our measured flow at Black Sand of 460 L/s, this temperature anomaly corresponds to a heat output of 4 MW. Big Springs, the largest spring in the region with a constant flow of about 6000 L/s represents a heat output of 110 MW. The combined output of anomalous Cl in Black Sand and Big Springs is ~ 20 g/s, assuming a background concentration of 0.5 mg/L. The combined output of magmatic C is ~ 5.4 tonnes/day (20 tonnes/day expressed as CO_2) based on the $C_{(\text{dead})}$ values in Table 2.

Due to their large discharge, the heat and mass output of these two low-temperature springs is actually greater than that of most large hot springs. Terrace Spring, for example, discharges 20 MW of heat, 5.8 g/s of Cl, and 3.1 tonnes/day of magmatic C (11.4 tonnes/day as CO_2) including that released as diffuse emissions from soil around the spring (Lowenstern et al., 2005). Important to this study, however, is that the anomalous heat and mass output in Black Sand and Big Springs is very small in comparison to the respective totals for Yellowstone discussed above (6100 MW heat, 1740 g/s hydrothermal Cl, 45,000 tonnes/day magmatic CO_2).

4.5. Fluids, seismicity, and deformation

Waite and Smith (2002) discuss the problems in modeling the 1985 seismic swarm as a magmatic intrusion and favor seismic propagation being driven by hydrothermal fluids. Such fluids—brines or vapors—escaping from the caldera at seismogenic depths should have high concentrations of magmatic gases such as CO_2 and ^3He . Linking both the 1985 seismic swarm and the change in deformation that same year to fluid flow (Waite and Smith, 2002) implies that the flow rate was sufficiently voluminous to effect caldera subsidence. The geochemical signal expected from such an event would be a substantial pulse of gas or gas-rich thermal water. What our spring sampling revealed was a weak signal of magmatic gas associated with relatively gas-depleted thermal water, and both of insignificant proportions compared to the total outputs of gas and thermal water from Yellowstone.

Favara et al. (2001) describe a strong but short-lived CO_2 anomaly following a seismic sequence in Italy. Our survey, conducted nearly 20 years after the 1985 swarm, would have missed any short-lived geochemical anomaly in the springs. However, samples of both Black Sand and Big Springs collected in 1990 and 1991, just a few

years after the 1985 swarm and during the ensuing 10-year period of caldera subsidence, show similar specific conductance and major-ion chemistry to what we found (Kharaka et al., 2002). Unpublished pre-1985 data on Big Springs, the site of a former USGS gage, includes occasional measurements of temperature and conductance that extend back many decades. The similarity between our data and these pre-1985 results that include a $^3\text{He}/^4\text{He}$ ratio of $1.39R_A$ in 1983 (B.M. Kennedy, personal communication) suggests that the anomalies we observed are for the most part long-term characteristics, not specifically associated with the 1985 swarm. Overall, the spring data are consistent with long-term leakage of depressurized and boiled water out of Yellowstone into the study area.

Large amounts of fluid are not required for seismic swarm propagation as long as sufficient fluid is present to pressurize the fractures (as discussed by Waite and Smith, 2002). The spring geochemistry provides no evidence for major leakage of high-pressure fluid along the path of the 1985 seismic swarm, and suggests that other causes for the 10-year period of caldera subsidence should be considered. Subsidence actually seems to have begun prior to the seismic swarm (Dzurisin et al., 1994). Both events may be effects of some other perturbation, such as movement of magma beneath the caldera or the Norris-Mammoth corridor (Wicks et al., 1998, 2002), or major fluid leakage elsewhere, including vertical leakage of magmatic brines and gases within the caldera.

The concept of episodic leaks of hydrothermal fluids through breaks in a self-sealed zone of mineral deposition was discussed by Fournier (1989), who proposed that inside the caldera, leaks that are large enough to cause subsidence might result only in a change in vapor and liquid proportions within the vapor-dominated part of the system. In this scenario, layering of the brine beneath the vapor cap could explain why conspicuous changes in total Cl discharge in rivers have not been observed in concert with inflation-deflation cycles (Ingebritsen et al., 2001; Fournier, 2004). However, due to its low solubility in water at high temperatures, CO_2 would not be trapped in the liquid phase, and breaching of the self-sealed zone should result in large increases in gas emission rate within the caldera. A linkage between multi-year cycles of caldera deformation and enhanced emission of CO_2 has been well documented at Phlegrean Fields caldera in Italy (Chiodini et al., 2003).

The seeming disconnect between our geochemical results (little CO_2 anomaly in groundwaters) and seismic tomography (large quantity of free gas at shallow depths in faulted terrain) must be discussed regardless of the

sources of seismicity and deformation. Seismic tomography has proven useful at imaging gas and vapor zones elsewhere, even revealing gas migration in a study (Foulger et al., 2003) at Mammoth Mountain volcano where CO₂-rich springs are numerous. A large, permeable gas reservoir several km in vertical extent (as imaged by Husen et al., 2004) implies an internal pressure gradient much different from regional hydrostatic or lithostatic gradients, and in this area of frequent seismicity, would be expected to leak (see Holloway et al., 2005). The lack of significant anomalies in springs within or near the area overlying the gas reservoir, or in streams draining this area, could be indicative of low permeability in that part of the reservoir that extends into the study area (Fig. 1). However, low permeability is difficult to reconcile with the high reservoir porosity (~0.1) proposed by Husen et al. (2004). Low permeability would also work against a scenario in which large, rapid inflows of Yellowstone-source fluids (i.e. in 1985) could be easily stored at depth and not forced to the surface.

5. Conclusions

Our survey of waters northwest of the Yellowstone caldera identified two large-discharge springs that contain a component of thermal fluid as shown by magmatic He and C, elevated concentrations of Cl, and warmer than normal temperatures. However, the geochemical anomalies appear to be long-lived characteristics without obvious relation to the 1985 seismic swarm. In addition, the anomalies reflect gas-depleted fluids compared to the expected deep parent fluid composition in the Yellowstone system, and certainly cannot be linked to a pulse of gassy fluid from the 1985 swarm. Springs and streams draining the northwest rim of the caldera (Fig. 1) show no sign of CO₂ leaking upward to the surface from the imaged gas reservoir of Husen et al. (2004), requiring that this part of the gas reservoir be extremely tight despite its high imaged porosity.

Our results are compatible with the involvement of pressurized hydrothermal fluids in the 1985 swarm, but they suggest that if caldera subsidence resulted from large-scale fluid leakage, the fluid mostly escaped elsewhere. An intense but short-lived geochemical anomaly cannot be ruled out, given the timing of sampling surveys, but other potential fluid flow paths that might be active during caldera subsidence at Yellowstone need further investigation. We suggest that intracaldera CO₂ efflux, which is currently unmonitored apart from the one-time survey of Werner

and Brantley (2003), might track caldera deformation cycles even if riverine Cl does not.

Acknowledgements

We thank Christie Hendrix (NPS) for logistical help within the park and the Reston Stable Isotope Laboratory (USGS) for analytical support. Kathryn Flynn (USGS) provided GIS expertise for the construction of Fig. 1, and James Montesi (USDA) provided SNOTEL data. Lizet Christiansen helped with the sampling. Jake Lowenstern, Jen Lewicki, Cindy Werner, and Fraser Goff provided constructive reviews.

References

- Amundson, R.G., Davidson, E.A., 1990. Carbon dioxide and nitrogenous gases in the soil atmosphere. In: Kessler, S.E. (Ed.), *Soil and Rock Gas Geochemistry*. J. Geochem. Explor., vol. 38, pp. 13–41.
- Bräuer, K., Kämpf, H., Strauch, G., Weise, S.M., 2003. Isotopic evidence (³He/⁴He, ¹³C_{CO2}) of fluid triggered intraplate seismicity. J. Geophys. Res. 108 (B2), doi:10.1029/2002JB002077.
- Chiodini, G., Frondini, F., Kerrick, D.M., Rogie, J., Parello, F., Peruzzi, L., Zanzari, A.R., 1999. Quantification of deep CO₂ fluxes from Central Italy. Examples of carbon balance for regional aquifers and of soil diffuse degassing. Chem. Geol. 159, 205–222.
- Chiodini, G., Todesco, M., Caliro, S., Del Gaudio, C., Macedonio, G., Russo, M., 2003. Magma degassing as a trigger of bradyseismic events: the case of Phlegrean Fields (Italy). Geophys. Res. Lett. 30 (8), doi:10.1029/2002GL016790.
- Chiodini, G., Cardellini, C., Amato, A., Boschi, E., Caliro, S., Frondini, F., Ventura, G., 2004. Carbon dioxide Earth degassing and seismogenesis in central and southern Italy. Geophys. Res. Lett. 31 (7), doi:10.1029/2004GL019480.
- Christiansen, R.L., 2001. The Quaternary and Pliocene Yellowstone Plateau volcanic field of Wyoming, Idaho, and Montana. U. S. Geol. Surv. Prof. Pap. 729-G (145 pp.).
- Cruz, J.V., Coutinho, R.M., Carvalho, M.R., Oskarsson, N., Gislason, S.R., 1999. Chemistry of waters from Furnas volcano, São Miguel, Azores: fluxes of volcanic carbon dioxide and leached material. J. Volcanol. Geotherm. Res. 92, 151–167.
- Despain, D.G., 1987. The two climates of Yellowstone National Park. Proc. Mont. Acad. Sci. 47, 11–20.
- Dzurisin, D., Yamashita, K.M., Kleinman, J.W., 1994. Mechanisms of crustal uplift and subsidence at the Yellowstone caldera, Wyoming. Bull. Volcanol. 56, 261–270.
- Evans, W.C., Sorey, M.L., Cook, A.C., Kennedy, B.M., Shuster, D.L., Colvard, E.L., White, L.D., Huebner, M.A., 2002. Tracing and quantifying magmatic carbon discharge in cold groundwaters: lessons learned from Mammoth Mountain, USA. J. Volcanol. Geotherm. Res. 114, 291–312.
- Evans, W.C., van Soest, M.C., Mariner, R.H., Hurwitz, S., Ingebritsen, S.E., Wicks Jr., C.W., Schmidt, M.E., 2004. Magmatic intrusion west of three sisters, central Oregon, USA: the perspective from spring geochemistry. Geology 32, 69–72.
- Farrar, C.D., Sorey, M.L., Evans, W.C., Howle, J.F., Kerr, B.D., Kennedy, B.M., King, C.-Y., Southon, J.R., 1995. Forest-killing

- diffuse CO₂ emission at Mammoth Mountain as a sign of magmatic unrest. *Nature* 376, 675–678.
- Favara, R., Italiano, F., Martinelli, G., 2001. Earthquake-induced chemical changes in the thermal waters of the Umbria region during the 1997–1998 seismic swarm. *Terra Nova* 13, 227–233.
- Foulger, G.R., Julian, B.R., Pitt, A.M., Hill, D.P., Malin, P.E., Shalev, E., 2003. Three-dimensional crustal structure of Long Valley caldera, California, and evidence for the migration of CO₂ under Mammoth Mountain. *J. Geophys. Res.* 108 (B3), doi:10.1029/2000JB000041.
- Fournier, R.O., 1989. Geochemistry and dynamics of the Yellowstone National Park hydrothermal system. *Annu. Rev. Earth Planet. Sci.* 17, 13–53.
- Fournier, R.O., 2004. Yellowstone caldera inflation-deflation and hydrothermal Cl flux revisited. In: Wanty, R.B., Seal III, R.R. (Eds.), *Proc. 11th International Symposium on Water–Rock Interaction*. A.A. Balkema, Leiden, pp. 53–58.
- Friedman, I., 1970. Some investigations of the deposition of travertine from Hot Springs-I. The isotope chemistry of a travertine-depositing spring. *Geochim. Cosmochim. Acta* 34, 1303–1315.
- Hildreth, W., Halliday, A.N., Christiansen, R.L., 1991. Isotopic and chemical evidence concerning the genesis and contamination of basaltic and rhyolitic magma beneath the Yellowstone Plateau volcanic field. *J. Petrol.* 32, 63–138.
- Hill, D.P., Prejean, S., 2005. Magmatic unrest beneath Mammoth Mountain, California. *J. Volcanol. Geotherm. Res.* 146, 257–283.
- Hilton, D.R., Fischer, T.P., Marty, B., 2002. Noble gases and volatile recycling at subduction zones. In: Porcelli, D., Ballentine, C.J., Wieler, R. (Eds.), *Noble Gases in Geochemistry and Cosmochemistry*. *Rev. Mineral. Geochem.*, vol. 47, pp. 319–370.
- Hiyagon, H., Kennedy, B.M., 1992. Noble gases in CH₄-rich gas fields, Alberta, Canada. *Geochim. Cosmochim. Acta* 56, 1569–1589.
- Holloway, S., Pearce, J.M., Ohsumi, T., Hards, V.L., 2005. A review of natural CO₂ occurrences and their relevance to CO₂ storage. BGS External Report CR/05/104, 117 pp.
- Husen, S., Smith, R.B., Waite, G.P., 2004. Evidence for gas and magmatic sources beneath the Yellowstone volcanic field from seismic tomographic imaging. *J. Volcanol. Geotherm. Res.* 131, 397–410.
- Ingebritsen, S.E., Galloway, D.L., Colvard, E.M., Sorey, M.L., Mariner, R.H., 2001. Time-variation of hydrothermal discharge at selected sites in the western United States: implications for monitoring. *J. Volcanol. Geotherm. Res.* 111, 1–23.
- James, E.R., Manga, M., Rose, T.P., 1999. CO₂ degassing in the Oregon Cascades. *Geology* 27, 823–826.
- Kennedy, B.M., Lynch, M.A., Reynolds, J.H., Smith, S.P., 1985. Intensive sampling of noble gases in fluids at Yellowstone: I. Early overview of the data, regional patterns. *Geochim. Cosmochim. Acta* 49, 1251–1261.
- Kennedy, B.M., Reynolds, J.H., Smith, S.P., Truesdell, A.H., 1987. Helium isotopes: lower Geyser Basin, Yellowstone National Park. *J. Geophys. Res.* 92, 12477–12489.
- Kharaka, Y.K., Thordsen, J.J., White, L.D., 2002. Isotopic and chemical compositions of meteoric and thermal waters and snow from the greater Yellowstone National Park region. *Open-File Rep. (U. S. Geol. Surv.)* 02-194 (18 pp.).
- Lowenstem, J.B., Evans, W.C., Bergfeld, D., 2005. Diffuse and direct sources of CO₂ from Terrace Spring, a large-volume travertine-forming spring at Yellowstone National Park. *IAVCEI Gas Workshop Abstracts, Italy*. 1 p.
- Manga, M., 2001. Using springs to study groundwater flow and active geologic processes. *Annu. Rev. Earth Planet. Sci.* 29, 201–228.
- Miller, S.A., Collettini, C., Chlaraluce, L., Cocco, M., Barchi, M., Kaus, B.J.P., 2004. Aftershocks driven by a high-pressure CO₂ source at depth. *Nature* 427, 724–727.
- Nathenson, M., Thompson, J.M., White, L.D., 2003. Slightly thermal springs and non-thermal springs at Mount Shasta, California: chemistry and recharge elevations. *J. Volcanol. Geotherm. Res.* 121, 137–153.
- O'Neill, J.M., Christiansen, R.L., 2004. Geologic map of the Hebgen Lake Quadrangle, Beaverhead, Madison, and Gallatin Counties, Montana, Park and Teton Counties, Wyoming, and Clark and Fremont Counties, Idaho. *U.S. Geol. Surv. Sci. Inv. Map* 2816, 1 p.
- Parry, W.T., Bowman, J.R., 1990. Chemical and stable isotopic models for Boundary Creek warm springs, southwestern Yellowstone National Park, Wyoming. *J. Volcanol. Geotherm. Res.* 43, 133–157.
- Pearson, F.J., Truesdell, A.H., 1978. Tritium in waters of Yellowstone National Park. *Open-File Rep. (U. S. Geol. Surv.)* 78-701, 327–329.
- Pelton, J.R., Smith, R.B., 1982. Contemporary vertical surface displacements in Yellowstone National Park. *J. Geophys. Res.* 87, 2745–2761.
- Plummer, L.N., Busby, J.F., Lee, R.W., Hanshaw, B.B., 1990. Geochemical modeling of the Madison Aquifer in parts of Montana, Wyoming, and South Dakota. *Water Resour. Res.* 26, 1981–2014.
- Saar, M.O., Castro, M.C., Hall, C.M., Manga, M., Rose, T.P., 2005. Quantifying magmatic, crustal, and atmospheric helium contributions to volcanic aquifers using all stable noble gases: implications for magmatism and groundwater flow. *Geochem. Geophys. Geosyst.* 6 (3), doi:10.1029/2004GC000828.
- Sorey, M.L., 1991. Effects of potential geothermal development in the Corwin Springs Known Geothermal Resources Area, Montana, on the thermal features of Yellowstone National Park. *U. S. Geol. Surv. Water Resour. Invest. Rep.* 91-4052 (195 pp.).
- Sorey, M.L., Evans, W.C., Kennedy, B.M., Farrar, C.D., Hainsworth, L.J., Hausback, B., 1998. Carbon dioxide and helium emissions from a reservoir of magmatic gas beneath Mammoth Mountain, California. *J. Geophys. Res.* 103, 15303–15323.
- Waite, G.P., Smith, R.B., 2002. Seismic evidence for fluid migration accompanying subsidence of the Yellowstone caldera. *J. Geophys. Res.* 107 (B9), doi:10.1029/2001JB000586.
- Werner, C., Brantley, S., 2003. CO₂ emissions from the Yellowstone volcanic system. *Geochem. Geophys. Geosyst.* 4 (7), doi:10.1029/2002GC000473.
- Wicks Jr, C.W., Thatcher, W., Dzurisin, D., 1998. Migration of fluids beneath Yellowstone caldera inferred from satellite radar interferometry. *Science* 282, 458–462.
- Wicks Jr, C.W., Thatcher, W., Dzurisin, D., 2002. Satellite InSAR reveals a new style of deformation at Yellowstone caldera. *EOS Trans. AGU* 83, F1348.
- Wilhelm, E., Battino, R., Wilcock, R.J., 1977. Low-pressure solubility of gases in liquid water. *Chem. Rev.* 77, 219–262.